Sequential Therapy With JX-594, A Targeted Oncolytic Poxvirus, Followed by Sorafenib in Hepatocellular Carcinoma: Preclinical and Clinical Demonstration of Combination Efficacy

Jeong Heo[1], Caroline J Breitbach[2], Anne Moon[2], Chang Won Kim[1], Rick Patt[3], Mi Kyung Kim[1], Yu Kyung Lee[1], Sung Yong Oh[4], Hyun Young Woo[1], Kelley Parato[5], Julia Rintoul[5], Theresa Falls[5], Theresa Hickman[2], Byung-Geon Rhee[6], John C Bell[2,5], David H Kirn[2] and Tae-Ho Hwang[1]

[1]Pusan National University, Busan, South Korea; [2]Jennerex Inc., San Francisco, California, USA; [3]RadMD, Doylestown, Pennsylvania, USA; [4]Dong-A University, Busan, South Korea; [5]Ottawa Hospital Research Institute and University of Ottawa, Ottawa, Ontario, Canada; [6]Green Cross Corp., Yongin, South Korea

JX-594 is a targeted and granulocyte-macrophage colony stimulating factor (GM-CSF) expressing oncolytic poxvirus designed to selectively replicate in and destroy cancer cells through viral oncolysis and tumor-specific immunity. In a phase 1 trial, JX-594 injection into hepatocellular carcinoma (HCC) was well-tolerated and associated with viral replication, decreased tumor perfusion, and tumor necrosis. We hypothesized that JX-594 and sorafenib, a small molecule inhibitor of B-raf and vascular endothelial growth factor receptor (VEGFR) approved for HCC, would have clinical benefit in combination given their demonstrated efficacy in HCC patients and their complementary mechanisms-of-action. HCC cell lines were uniformly sensitive to JX-594. Anti-raf kinase effects of concurrent sorafenib inhibited JX-594 replication *in vitro*, whereas sequential therapy was superior to either agent alone in murine tumor models. We therefore explored pilot safety and efficacy of JX-594 followed by sorafenib in three HCC patients. In all three patients, sequential treatment was (i) well-tolerated, (ii) associated with significantly decreased tumor perfusion, and (iii) associated with objective tumor responses (Choi criteria; up to 100% necrosis). HCC historical control patients on sorafenib alone at the same institutions had no objective tumor responses (0 of 15). Treatment of HCC with JX-594 followed by sorafenib has antitumoral activity, and JX-594 may sensitize tumors to subsequent therapy with VEGF/VEGFR inhibitors.

INTRODUCTION

The targeted oncolytic poxvirus JX-594 replicates selectively in cancer cells resulting in virus progeny production, tumor cell necrosis (oncolysis), JX-594 release and subsequent spread within tumor tissues.[1] JX-594 is also engineered to express the granulocyte-macrophage colony stimulating factor (GM-CSF) transgene, a potent activator of dendritic cells,[2] in order to enhance the antitumor immunity that results from oncolysis. In addition, JX-594 and other oncolytic poxviruses and vesicular stomatitis virus have been shown to trigger an acute reduction in tumor perfusion in mouse models.[3,4] Therefore, JX-594 is able to induce direct viral oncolysis followed by tumor vascular shutdown and antitumoral immunity. The Wyeth vaccinia backbone of JX-594 is inherently tumor-selective due to endothelial growth factor receptor (EGFR)-ras pathway dependency (activated in cancer cells)[5,6] and resistance to interferon induction and effects in tumors.[7] The inherent therapeutic index is amplified by the deletion of the vaccinia thymidine kinase (*TK*) gene. As a result, JX-594 replication is also dependent on high levels of cellular TK which is driven by cell cycle abnormalities in cancer.[8] Results from a phase 1 clinical trial of intratumoral JX-594 in patients with refractory liver tumors demonstrated safety, antitumor efficacy and mechanistic proof-of-concept for JX-594 replication, systemic dissemination to distant tumors and expression of biologically active GM-CSF.[9] In this trial, hepatocellular carcinoma (HCC) were found to be highly sensitive to JX-594, resulting in acute vascular shutdown and necrotic (Choi) tumor responses.[10] Noninjected tumors also demonstrated infection and necrosis following trafficking of JX-594 through the blood to distant tumor sites. No liver toxicity was reported. Phase 2 development of JX-594 in patients with advanced HCC was therefore indicated.

The only approved systemic therapy for HCC to date is sorafenib (Nexavar, and Bayer, Leverkusen, Germany). Sorafenib is an oral small molecule multi-kinase inhibitor that has both antiproliferative (*via* B-raf kinase inhibition) and antiangiogenic effects [*via* inhibition of vascular EGFR (VEGFR)] in mice and humans.[11] Sorafenib was evaluated in two phase 3 randomized clinical trials of patients with advanced HCC.[12,13] In both of these trials, objective tumor responses were rare (1–2% objective partial Response

Evaluation Criteria In Solid Tumors (RECIST) responses). The median survival duration was increased by ~3 months. Sorafenib toxicities include rash (hand-foot syndrome), diarrhea, and fatigue; dose reductions and/or discontinuation are common. Therefore, novel therapies are needed for patients with HCC, both as single agents and in combination with sorafenib therapy.

We hypothesized that the combination of the oncolytic poxvirus JX-594 and the small molecule sorafenib could result in superior efficacy to that achievable with sorafenib alone in HCC. These agents have differing and complementary mechanisms-of-action. JX-594 induces acute tumor cell cytolysis, tumor vascular disruption, and necrosis followed by long-term antitumor immunity. In contrast, sorafenib is antiangiogenic and inhibits tumor progression. In addition, the toxicity profiles are not overlapping, and therefore the combination was predicted to have an acceptable toxicity profile. A potential problem with this combination, if given simultaneously, would be that sorafenib could block JX-594 replication through its raf inhibition. We explored simultaneous and sequential combinations *in vitro* and in animal tumor models. Based on promising preclinical data with sequential treatment, clinical proof-of-concept was explored in HCC patients who had completed JX-594 treatment as a single agent on a phase 2 trial. After progression following JX-594, standard sorafenib therapy was evaluated in these patients. In order to assess whether the findings in JX-594 treated patients were typically seen with sorafenib alone, the effect of sorafenib

alone was assessed in concurrent and recent historical controls at the same institutions. Finally, a renal cell carcinoma patient was treated with JX-594 followed by sunitinib (Sutent, Pfizer, New York, NY), another small molecule inhibitor of VEGFR with an activity profile similar to sorafenib. Renal cell cancer (RCC) is similar to HCC in that it is a highly vascularized tumor type, and sunitinib shares similar VEGFR inhibition with sorafenib. Therefore, this RCC patient shares similar histologic and treatment features to the three HCC patients.

RESULTS
Sorafenib inhibits JX-594 replication *in vitro*
Based upon our earlier clinical studies[9] we predicted that JX-594 would be able to infect and kill a wide variety of cell lines derived from human HCC. Indeed we found that JX-594, *in vitro*, infects and destroys several different human HCC cell lines. HepG2, SNU423, SNU475, SNU449, and PLC/PRF/5 have been tested and shown to be susceptible to JX-594 infection by burst and/or plaque assay (**Figure 1a–e**). In addition, the ability of a sorafenib resistant/adapted derivative of PLC/PRF/5 to support JX-594 replication was evaluated. To generate sorafenib resistant/adapted cultures, PLC/PRF-5 cells were grown *in vitro* at increasing doses of sorafenib for a total of 3 months, starting at a sorafenib concentration of 1 μmol/l and increasing up to 6 μmol/l. The resistant/adapted cells supported JX-594 replication at a level comparable to its parental sorafenib sensitive clone (**Figure 1a**). As discussed earlier, the
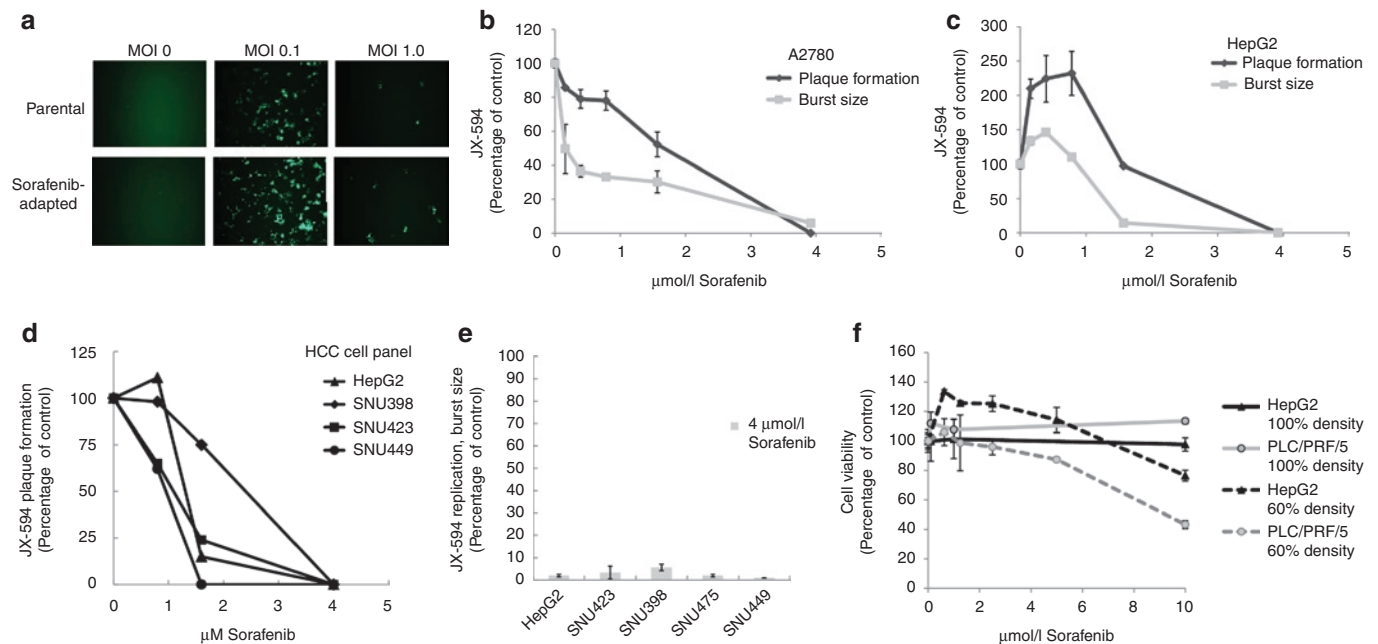
Figure 1 JX-594 replication in liver cancer lines is inhibited in the presence of sorafenib *in vitro*. (a) Infectability of PLC/PRF/5 (human hepatoma) cells (parental) and sorafenib-adapted PLC/PRF/5 cells was determined by addition of JX-594 expressing green fluorescent protein at multiplicities of infection (MOI) of 0, 0.1 and 1. Images were taken with a Zeiss Axiovision microscope fluorescent microscope and analyzed using Axiovision acquisition and image storage software 24 hours postinfection. (**b,c**) JX-594 replication in the presence of sorafenib was measured by plaque formation and burst assay after incubation with sorafenib for 3 days (plaque formation assay) or 24 hours (burst assay). Results are expressed as percent of no-sorafenib control (replicate mean + SD). (**d**) The ability of JX-594 to form plaques in the absence or presence of increasing concentrations of sorafenib on monolayers of hepatocellular carcinoma (HCC) cell lines. Results are expressed as percent of no sorafenib control. (**e**) JX-594 replication was tested by burst assay using a panel of HCC cell lines infected at MOI of 0.1 for 2 hours, followed by change to media with 4 μmol/l sorafenib. After 48 hours, cells and supernatants were collected for titration by plaque assay on A2780 cells. Results are expressed as percent of no-sorafenib control (replicate mean + SD). (**f**) Cell viability in the presence of sorafenib was determined 24 hours after addition of sorafenib to PLC/PRF/5 and HepG2 cells plated at 60% and 100% densities. Results are expressed as percent of no-sorafenib control (replicate mean + SD).

replication of JX-594 is determined in part by activation of the EGFR/Ras/Raf pathway and so we reasoned that as a Raf kinase inhibitor, sorafenib might theoretically affect virus replication. We therefore tested the ability of JX-594 to infect and replicate tumor cells in the presence of sorafenib. JX-594 was allowed to infect monolayers of A2780 (ovarian cancer cell line) or HepG2 (HCC cell line) in the absence or presence of increasing concentrations of sorafenib, and JX-594 replication was assessed by measuring plaque formation on the original monolayer, and the production of new plaque-forming units (pfu, replicative burst) (**Figure 1b,c**). JX-594 plaque formation and replication were inhibited in a dose-related fashion (**Figure 1b,c**); inhibition was >95% at 4 µmol/l sorafenib. Similar results were found in a subsequent experiments using a broader panel of HCC cell lines (**Figure 1d,e**) and PLC/PRF/5 cells (data not shown), JX-594 plaque formation was inhibited in the presence of sorafenib in a dose-dependent fashion (**Figure 1e**), and JX-594 replication as measured by burst assay was decreased by >90% in all cases by sorafenib concentrations of 4 µmol/l (**Figure 1e**). The concentrations of sorafenib shown to inhibit JX-594 replication (*e.g.*, 4 µmol/l) were shown to be noncytocidal in a sorafenib-alone condition; cells plated at 100% and incubated with sorafenib for 24 hours did not have reduced viability compared to no-sorafenib control. Cells plated at 60% density and incubated with sorafenib for 24 hours also showed no cytotoxicity at 5 µmol/l, while higher concentrations were grown-inhibitory as demonstrated by the 10 µmol/l sorafenib condition that did grow out compared to control at 24 hours (**Figure 1f**). Thus as predicted, the raf kinase inhibitor sorafenib significantly decreased JX-594 replication on viable tumor cells.

Sequential combination of JX-594 and sorafenib results in improved efficacy in two murine tumor models

The data presented above demonstrated that JX-594 efficiently infects HepG2 cells *in vitro* and therefore a murine xenograft model was established using this cell line to evaluate the use of sorafenib in combination with JX-594 *in vivo*. In order to be able to detect additive/synergistic effects when JX-594 and sorafenib were administered simultaneously both agents were given at doses that were suboptimal as single agents in this model. Our pilot experiments showed that doses of 500 µg and 1,000 µg sorafenib/day intraperitoneally in mice resulted in plasma concentrations of ~0.9 mg/l and ~3.1 mg/l (data not shown). Therefore, the doses of sorafenib used in this study were clinically relevant and had detectable effects in this model.

Tumors in control animals treated daily with phosphate-buffered saline (PBS) progressed rapidly, reaching a mean size of 10,000 mm³ on day 25. Sorafenib or JX-594 dosing alone slowed tumor growth. By the end of study on day 31, the JX-594 group showed significant inhibition versus the PBS control group whereas the sorafenib group did not (*P* values of 0.0005 and 0.3693, respectively; paired Student's *t*-test). The regimen of JX-594 followed by sorafenib was statistically superior to PBS (*P* value 0.0028) and sorafenib alone (*P* value 0.0101) in terms of tumor growth at the end of study on day 31. In addition, this sequence was superior to sorafenib followed by JX-594 (*P* value 0.0021) and to simultaneous treatment (*P* value 0.0052).

The time-to-tumor progression (TTP) was assessed according to Kaplan–Meier analysis (end point reached when tumors reached 5,000 mm³; log-rank test applied). The regimen of JX-594 followed by sorafenib was statistically significantly superior to all other regimens in terms of TTP. The data was plotted as Kaplan–Meier curves following percent nonprogression over time (**Figure 2a,b**). Animals that died prior to tumors reaching 5,000 mm³, or did not reach 5,000 mm³ by the end of study (day 31) were censored when running log-rank (Mantel–Cox) test. The best combination regimen (JX-594 followed by sorafenib) is shown compared to single agents in **Figure 2a**, and to other suboptimal combination regimens in **Figure 2b**. The *P* values for JX-594 followed by sorafenib versus other groups were as follows: PBS (<0.0001), sorafenib alone (0.0012), JX-594 alone (0.0149), sorafenib followed by JX-594 (0.0001), and sorafenib simultaneously with JX-594 (0.0042). The median TTP for animals in the JX-594 followed by sorafenib group was not reached by the end of the study (day 31). Median TTP times for the other groups were 17 days (PBS), 22 days (JX-594 alone), 27 days (sorafenib alone), 26 days (sorafenib together with JX-594) and 26 days (sorafenib followed by JX-594).

The efficacy of JX-594 in combination with sorafenib was subsequently evaluated in a metastatic B16 melanoma model as it allows for precise quantitation of lung metastases, and the assessment of efficacy in a widely metastatic tumor model in an immunocompetent host. Given the rapidity of tumor progression in this model, it was not feasible to perform sequential therapy. Therefore, JX-594 and sorafenib simultaneous combination therapy was evaluated. Combination therapy resulted in a significant reduction in the mean number of B16 tumors in the lungs compared to PBS (*P* < 0.001), the JX-594 alone group (*P* = 0.05) or the sorafenib alone group (*P* = 0.002) (**Figure 2c**).

Efficacy with modified Choi tumor responses following sequential JX-594 and sorafenib therapy in patients with advanced HCC

Encouraged by the preclinical data above, as well as JX-594 clinical data (objective responses, prolonged survival) as a single agent in HCC, we evaluated the sequential administration of JX-594 followed by sorafenib in patients. Prior to a prospectively designed trial of sequential combination therapy in patients, we elected to study this regimen in pilot fashion to confirm its safety and potential efficacy. Since a JX-594 phase 2 single agent trial was underway in advanced HCC patients who had not received prior sorafenib, we were able to follow patient safety and tumor response on standard sorafenib once tumors progressed following JX-594. Three such patients were identified, and special consent was obtained to obtain serial magnetic resonance imaging (MRI) scans while on sorafenib therapy. These individuals had initially received three intratumoral injections of JX-594 (every 2 weeks) into intrahepatic tumors and were evaluated radiographically at week 8 (by dynamic MRI). After tumor progression following JX-594, these patients were treated with standard sorafenib (the standard treatment in this patient population) and subsequently evaluated for safety and efficacy based on serial dynamic MRI imaging while on sorafenib.

Previous trials with JX-594 have demonstrated reproducible induction of clinically significant tumor necrosis. Therefore, the
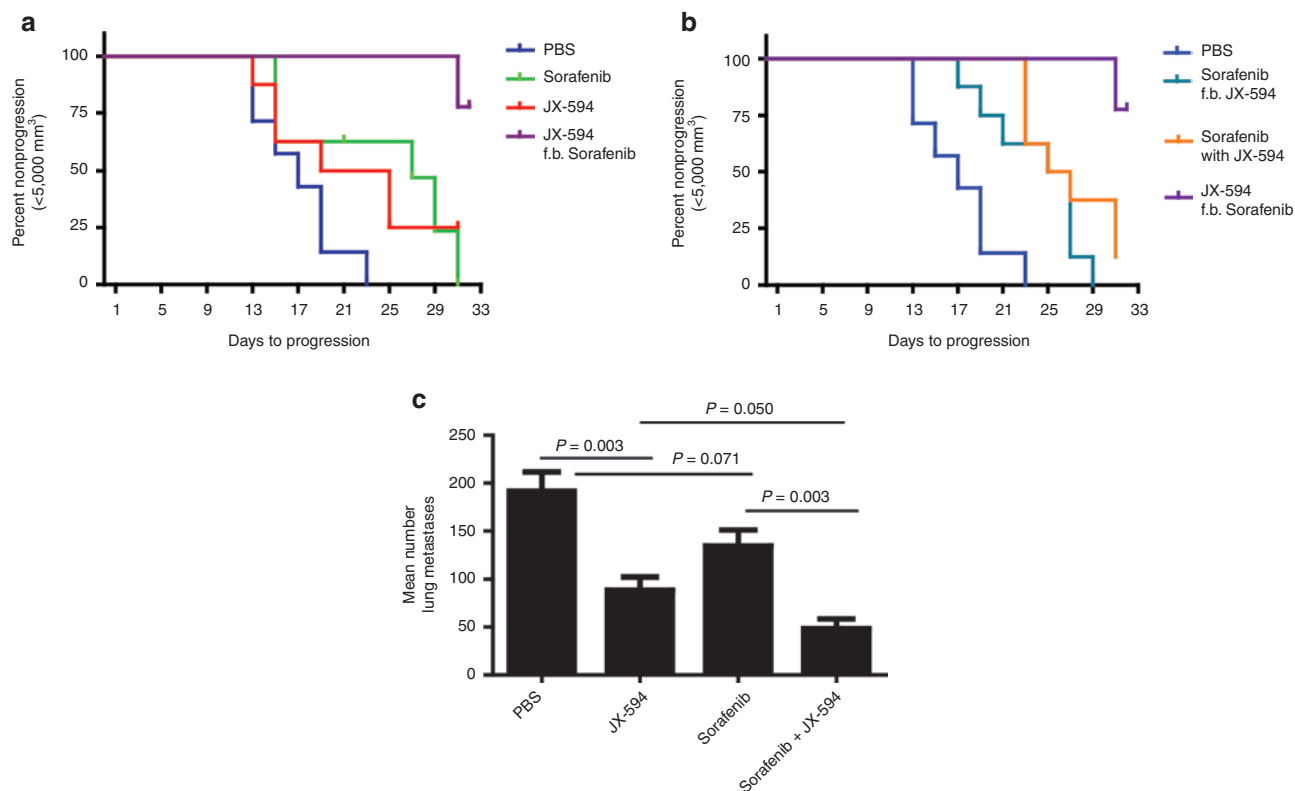
Figure 2 **Combination therapy with sorafenib enhances JX-594 efficacy in two murine tumor models.** (**a,b**) SCID mice with subcutaneous HepG2 tumors of 12–14 mm diameter were randomized to five groups and treated with PBS, daily sorafenib, weekly JX 594, simultaneous sorafenib and JX-594, or sequentially treated with sorafenib for 2 weeks followed by JX-594, or with 2 weekly dose of JX-594 followed by sorafenib. Analysis of time-to-tumor-progression (TTP) was performed. Kaplan–Meier curves show TTP, with 5,000 mm³ tumor volume considered as progression. (**c**) B16 model of lung metastases: C57BL/6 mice were injected with 3×10^5 B16-F10-LacZ cells intravenously and 24 hours later were treated with phosphate buffered saline (PBS), sorafenib alone (50 µg/kg per oral dosing daily for 2 weeks) JX594 alone (10^7 plaque-forming units (pfu) intravenously three times per week for 1 week) or in combination ($n = 5$ per group). Three weeks after treatment initiation, mice were killed and lungs were fixed and stained to detect surface B16 tumor nodules.

Choi criteria were deemed an appropriate method to assess antitumor activity of JX-594; Choi criteria are based on both tumor size and tumor enhancement (a measure of tumor perfusion and vascularity after intravenous contrast administration). In addition, the modified RECIST criteria for HCC were also utilized; these criteria were developed for HCC specifically by Lencioni *et al.*, and take into account changes in viable tumor size.[14] While on sorafenib all three patients exhibited rapid and marked tumor necrosis. Tumor necrosis was quantitated through serial measurement of tumor density (*i.e.*, decreased tumor contrast enhancement/ uptake over time) following initiation of sorafenib (**Figure 3a–c**) (**Table 1**). All patients had marked Choi responses[15] and modified RECIST-type responses.[14] Tumor responses on sorafenib occurred as early as 2.5 weeks after sorafenib initiation. In addition, one patient also had noninjected tumors within the liver, and marked tumor response following sorafenib was noted in these tumors as well as the injected tumors, consistent with known spread of JX-594 to noninjected tumors *via* the blood (**Figure 3c**); of note, noninjected tumor infection and responses were described with JX-594 in a phase 1 trial in liver tumor patients.[9] Also noteworthy is that sorafenib alone has not been described to induce Choi or modified RECIST (mRECIST) responses to date, although modest necrosis induction has been described in a minority of patients.[16]

Three-dimensional segmentation analysis of treated tumors reveals significant necrosis induction with JX-594 followed by sorafenib

In order to more fully understand the extent and distribution of tumor volume destruction, a three-dimensional (3D) segmentation analysis of liver tumors was performed in one patient (number 1705). MRI images at baseline, after JX-594 treatment alone (week 8) and post sorafenib initiation (week 13) (**Figure 3a**) were used to reconstruct the entire liver (both normal and tumor tissues) (**Figure 4a**). Necrosis induction was quantified and increasing volume of necrosis and decreasing volume of viable tumor were calculated within each tumors. In this patient, JX-594 treatment alone did not induce significant necrosis. However, following initiation of sorafenib, all three intrahepatic tumors became significantly necrotic (between 50 and 100% of the entire tumor volume) (**Figure 4b**).

Concurrent and historical control patients on sorafenib alone: lack of tumor responses

The relatively acute and extensive vascular disruption and tumor necrosis (captured as modified Choi tumor responses) described here with JX-594 followed by sorafenib has not been reported with sorafenib alone. Nevertheless, in order to assess whether sorafenib
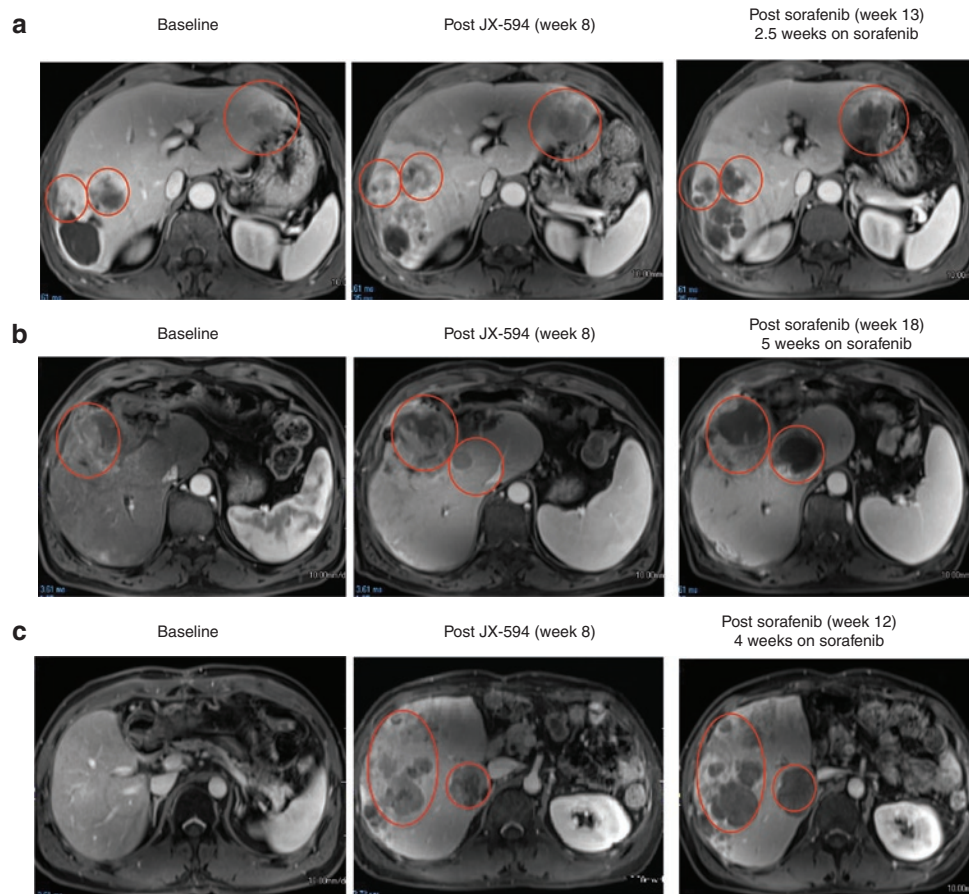
Figure 3 JX-594 treatment of patients with advanced hepatocellular carcinoma cell may sensitize to subsequent sorafenib therapy. (**a**) Patient 1705 was treated with JX-594 at a dose level of 10^8 plaque-forming units (pfu) intratumorally for three treatments every 2 weeks (week 0, week 2, week 4). Sorafenib therapy was initiated at week 10.5. Antitumor response was evaluated by dynamic contrast-enhanced magnetic resonance imaging (MRI) at baseline, after treatment with JX-594 alone and after sorafenib initiation. Red circles indicate target tumors. The darker areas within the target tumors at week 13 represent significant increasing necrosis within the target tumors is seen at week 11, manifested by nonenhancement within these tumors. (**b**) Patient 1702 was treated with JX-594 at a dose level of 10^9 pfu intratumorally for three treatments every 2 weeks (week 0, week 2, week 4). Sorafenib therapy was initiated at week 13. Response was evaluated by dynamic MRI imaging at baseline, after treatment with JX-594 alone and after sorafenib initiation. Red circles indicate target tumors. Mild amount of necrosis is seen in the larger tumor at baseline. The necrosis increases somewhat following JX-594 alone, but significant necrosis is identified following sorafenib therapy. (**c**) Patient 1712 was treated with JX-594 at a dose level of 10^9 pfu intratumorally for three treatments every 2 weeks (week 0, week 2, week 4). Sorafenib therapy was initiated at Week 8. Response was evaluated by dynamic MRI imaging at baseline, after treatment with JX-594 alone and after sorafenib initiation. Red ovals indicate areas of the liver not injected with JX-594. These images demonstrate antitumor activity in noninjected lesions similar to that seen in injected lesions from (**a**) and (**b**). Progressively developing necrosis within these tumors is seen following JX-594 therapy alone and then sorafenib.
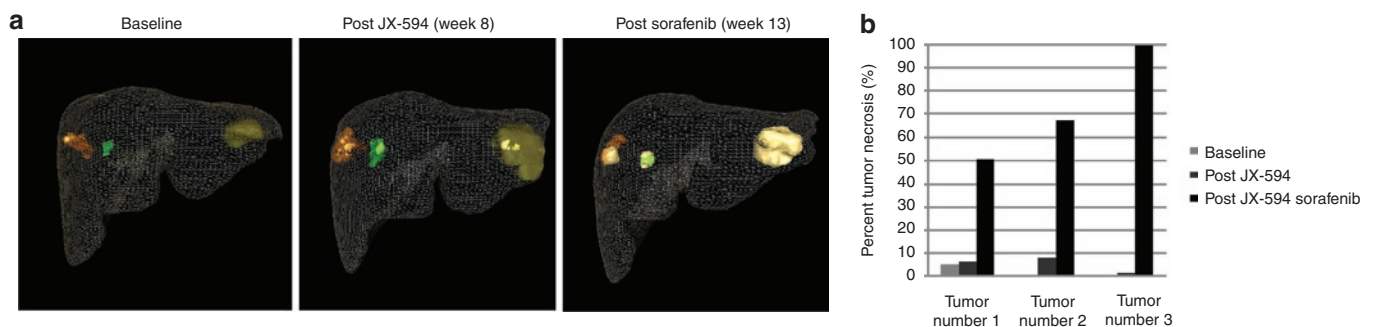
Figure 4 Three-dimensional segmentation analysis reveals significant tumor necrosis induction following JX-594 and sorafenib combination treatment. (**a**) Patient 1705 dynamic magnetic resonance imaging scans collected at baseline, week 8, and week 13 were evaluated using 3D segmentation analysis to assess the volumes of viable and necrotic tumor at each timepoint. Dark orange, green, and yellow indicate viable tumor tissue. Lighter colors within each tumor indicate geographic areas of necrosis. The liver margin is displayed as a wire frame. Note that on the week 13 image, the viable tumor in the largest lesion has been nearly completely replaced by necrosis. (**b**) Percent tumor necrosis (compared to total tumor volume) at baseline, after JX-594 therapy alone and after subsequent sorafenib initiation by tumor.

Table 1 Patient baseline tumor characteristics, treatment, and radiographic response to JX-594 and subsequent sorafenib

Patient number/JX-594 dose (plaque-forming units (pfu))	Baseline tumor(s) max diameter (cm), enhancement	Week 8 response to JX-594 alone (dynamic magnetic resonance imaging (MRI))	Best response to subsequent sorafenib (dynamic MRI)	Sorafenib dosing details	Sorafenib-associated toxicities (possibly or probably related)
1702/(10^9)	7.2 cm total (one tumor); 12% enhancement	Injected tumor: SD (−) Choi response (29% increase enhancement) overall: PD	Overall: (+) Choi response (68% decrease enhancement); SD	400 mg po b.i.d.; decrease to 400 q.d. (2.7 months); discontinue (8 months).	grade 1 hand-foot skin reaction (7 weeks); grade 1 fatigue (4 days); grade 2 esophageal pain (9 days)
1705/(10^8)	8.2 cm total (three tumors); 179% enhancement	Injected tumor: (+) Choi response (36% decrease enhancement) overall: PD	Overall: (+) Choi response (75% decrease enhancement); SD	400 mg po b.i.d.; decrease to 400 q.d. (5.0 months); discontinue (6.5 months)	grade 1 hand-foot skin reaction (5 months); grade 1 diarrhea (5 days)
1712/(10^9)	11.8 cm total (four tumors); 120% enhancement	Injected tumor: (+) Choi response (33% decrease enhancement) overall: PD	Overall: (+) Choi response (89% decrease enhancement); SD	400 mg po b.i.d.; decrease to 400 q.d. (1.7 months); discontinue (2.5 months)	grade 1 hand-foot skin reaction (6 weeks)

Abbreviations: q.d., once daily; b.i.d., twice daily; PD, progressive disease by Response Evaluation Criteria In Solid Tumors (RECIST); po, per oral dosing; SD, stable disease by RECIST.
Choi response criteria: maximum diameter decrease of ≥10% or density decrease of ≥15%.

alone routinely induces modified Choi responses, HCC patients treated with sorafenib alone at the same institutions over the preceding two years (i.e., historical and concurrent) were assessed if they had serial dynamic MRI scans of the liver (baseline and at least one follow-up scan at week 8 or later). Fifteen consecutive control patients were identified. The Barcelona Clinic Liver Criteria (BCLC) stage, tumor stage, age and gender profiles were similar between control patients and those receiving JX-594 followed by sorafenib (**Table 1**). No modified Choi responses were evident in scans from these patients on sorafenib alone (**Table 2**). In addition, according to RECIST criteria,[17] while 9 of 15 (60%) patients had progressive disease as their best response on sorafenib alone (40% stable disease), no progressive disease was noted in the JX-594 treated sorafenib patients (three of three with stable disease).

Case report of a patient with RCC treated with JX-594 followed by sunitinib (small molecule inhibitor of VEGFR)

Given the potential for synergistic antitumor activity with JX-594 and sorafenib in patients with HCC, we evaluated sequential therapy with JX-594 followed by sunitinib (also a small molecule with VEGFR inhibitory properties as seen with sorafenib) that is approved for the treatment of RCC. RCC has a high degree of tumor vascularity, and is therefore highly similar to HCC in this feature. Therefore, this clinical situation is analogous to sorafenib therapy in HCC. A patient with metastatic RCC was treated with JX-594 on a phase 1 intratumoral dose escalation trial of JX-594. This patient had widely metastatic cancer, including a 14 cm abdominal mass. According to the prognostic criteria outlined by Patil *et al.*[18] the patient had poor prognosis disease and a life expectancy of <6 months. The patient received four injections of JX-594 into liver metastases, resulting in modified Choi tumor responses within the liver and abdomen, but massive bulky tumor
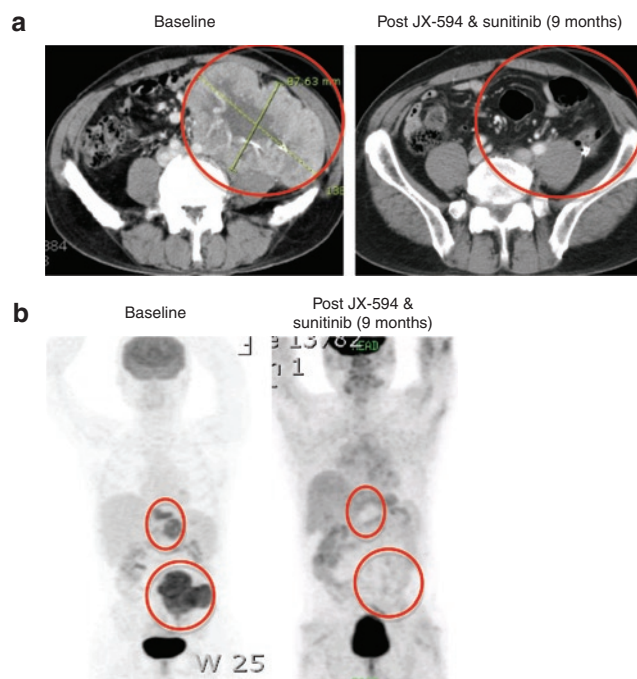
Figure 5 Tumor destruction in patient with advanced, poor prognosis renal cell cancer following JX-594 and sunitinib combination treatment. (a) Patient 301 was treated with JX-594 at a dose level of 10^9 plaque-forming units (pfu) intratumorally in liver metastases for four treatments every 3 weeks (week 0, week 3, week 6, and week 9). Sunitinib therapy was initiated at ~week 17. Contrast-enhanced computed tomography scans of patient 301 at baseline and 9 months after JX-594 and sunitinib treatment. A noninjected, large hypervascular mass in the left abdomen shows essentially complete resolution 9 months following JX-594 and sunitinib therapy. **(b)** Whole body positron emission tomography scan of patient at baseline and 9 months after JX-594 and sunitinib treatment shows complete disappearance of fludeoxyglucose-avid tumor following JX-594 and sunitinib.

Table 2 Hepatocellular carcinoma patients receiving sorafenib with (cases) or without (controls) prior JX-594: demographics, radiographic response to sorafenib by Response Evaluation Criteria In Solid Tumors (RECIST) and Choi criteria

Patient number	Age/ gender (F/M)	TNM stage	BCLC stage	Best response by RECIST	Best response by modified Choi
Controls					
1	51/F	4	C	PD	NR
2	48/M	4	C	SD	NR
3	57/M	2	B	SD	NR
4	43/F	3A	B	SD	NR
5	40/M	3A	C	SD	NR
6	63/M	1	A	SD	NR
7	55/M	1	A	PD	NR
8	67/M	3A	C	PD	NR
9	60/F	2	B	PD	NR
10	43/M	1	A	PD	NR
11	50/F	2	B	PD	NR
12	66/M	3A	C	PD	NR
13	56/M	3A	B	PD	NR
14	69/F	3A	C	SD	NR
15	67/M	2	B	PD	NR
Control totals				60% PD, 40% SD	0/15 Responses
JX-594-1	50/M	3A	C	SD	Response
JX-594-2	54/M	3A	C	SD	Response
JX-594-3	39/M	4	C	SD	Response
Cases totals				0% PD, 100% SD	3/3 Responses

Abbreviations: BCLC, Barcelona Clinic Liver Criteria; NR, nonresponder; PD, progressive disease by RECIST; SD, stable disease by RECIST.
Response/Choi response criteria: sum of diameters decrease of ≥10% or density decrease of ≥15%.

masses still remained. Sunitinib was initiated ~8 weeks after the last JX-594 dose. Therapy with full dose sunitinib (50 mg per day) was administered until dose reductions at 4 months (37.5 mg per day) and 7 months (25 mg); the patient remains on low dose sunitinib at this time. Despite the poor prognosis and significant dose reductions, the patient nevertheless exhibited a complete whole body tumor response by computed tomography and positron emission tomography scanning; this included complete disappearance of the large 14 cm. abdominal mass (**Figure 5a,b**). This patient remains alive and disease-free over 4 years after treatment initiation, despite a baseline life expectancy of <6 months.

DISCUSSION

We hypothesized that JX-594, a multi-mechanistic oncolytic poxvirus, and sorafenib, a small molecule inhibitor of both the B-raf kinase and VEGFR approved for advanced HCC treatment, would have efficacy in combination given their complementary and distinct mechanisms-of-action. Both agents have single agent activity in HCC, and their toxicities are not over-lapping. Here we report that sequential JX-594 followed by sorafenib in animal tumor

models was superior to either agent alone, despite inhibition of JX-594 replication by sorafenib if given simultaneously *in vitro*. Relevant syngeneic murine models of HCC are difficult to establish. In addition, JX-594 is derived from the Wyeth strain of vaccinia, a strain which demonstrates markedly lower replication in murine cells compared with human cells. Therefore, the efficacy of the two agents was first evaluated in a xenograft model of human HCC in which JX-594 replication and effects on tumor vasculature could be studied in the presence or absence of sorafenib. We subsequently elected to test the combination therapy in an immunocompetent murine tumor model (B16 lung metastases) that allowed for precise quantification of metastatic tumor burden (note: HCC in humans commonly metastasizes to the lungs). In addition to JX-594 replication and antivascular effects, the induction of potential antitumor immunity may be affected upon addition of sorafenib in this model, making it more relevant to subsequent human studies. The combination of JX-594 and sorafenib was superior to either agent alone in both models. In one model, simultaneous and sequential therapy could be evaluated. As expected in this human tumor model supporting robust viral replication, sequential therapy was superior to concurrent therapy (presumably due to inhibition of viral replication). In a murine tumor model in which viral replication effects are less relevant (JX-594 replication is markedly lower in murine tumor cells versus human tumor cells), concurrent therapy was superior to either agent alone.

Based on the preclinical data above, and single agent activity of both agents in HCC, we evaluated the sequential administration of JX-594 followed by sorafenib in patients. Since a JX-594 phase 2 single agent trial was underway in advanced HCC patients who had not received prior sorafenib, we were able to follow patient safety and tumor response on standard sorafenib once tumors progressed following JX-594. Three such patients were identified, and all three patients exhibited rapid (2.5 weeks) and marked tumor necrosis (up to 100% of the viable tumor mass) and responses on sorafenib. Of note, sorafenib alone has not been described to induce necrotic Choi or mRECIST responses to date, although modest necrosis induction has been described in a minority of patients.[16] Finally, 15 consecutive HCC historical and concurrent control patients on sorafenib alone at the same institutions were retrospectively assessed, and no Choi or mRECIST responses were noted (0 of 15). A fourth JX-594-treated patient (metastatic, poor prognosis RCC) from a separate phase 1 trial was treated with a similar small molecule angiogenesis inhibitor (sunitinib); this patient had a durable complete response lasting over 4 years (still on-going). JX-594 is expected to be cleared within weeks and dramatic responses in injected tumors long after completion of JX-594 therapy have not been observed to date. Therefore based on the data presented here, we hypothesize that JX-594 therapy may sensitize HCC tumors to sorafenib and potentially other VEGFR inhibitors (*i.e.*, a therapeutic class effect). A randomized controlled trial of sorafenib alone versus JX-594 followed by sorafenib is required to validate this hypothesis.

Additional nonclinical and clinical studies should be performed to confirm these findings. Only three patients were evaluated in this study; it is not yet clear whether these patients are representative of the HCC population at large. In addition, while mRECIST and Choi responses have not been reported

with sorafenib alone, it is possible that on future study sorafenib responses will be demonstrated. A phase 2 trial of JX-594 followed by sorafenib has been initiated in patients with advanced HCC. JX-594 treatment is followed by standard sorafenib initiated 1 week after the final JX-594 injection. Promising interim safety and efficacy data has been reported.[19] Of note, objective tumor responses have been reported for patients who have documented resistance to, and tumor progression on, sorafenib monotherapy. A prospective randomized trial will be required to confirm that JX-594 followed by sorafenib leads to superior response rate and survival duration compared to either agent alone in HCC patients; planning for such a trial is underway. In addition, if the ability of JX-594 to resensitize sorafenib-refractory tumors to sorafenib is confirmed, a randomized trial of JX-594 followed by sorafenib versus best supportive care may be indicated in this patient population. Similar trials can be envisioned with other inhibitors of the VEGFR pathway in development.

The potential mechanism(s) involved in JX-594-mediated sensitization of tumors to sorafenib remain to be elucidated. Of note, the effect(s) appear to occur relatively acute and durable, lasting up to 8 weeks or more following the last dose of JX-594 prior to sorafenib. We hypothesize that soluble mediators produced by residual cells within the tumor may be involved. Since sorafenib has effects on both tumor cells and their associated vasculature, it is possible that JX-594 sensitizes either or both of these tumor components to sorafenib. JX-594 replication and transgene expression within tumors may either decrease soluble factor(s) that are protective against sorafenib and/or increase concentrations of soluble sensitizers to sorafenib. It is known that the physiology of vascular endothelium can be affected by persistent epigenetic changes initiated by an acute event.[20,21] We hypothesize that cytokines released during JX-594 infection of tumors could reprogram vascular endothelial cells and render them exquisitely sensitive to the antiangiogenic properties of sorafenib for extended periods of time. Interestingly, it has been shown that the expression of the sorafenib target, VEGFR, is susceptible to epigenetic modulation through DNA methylation.[22] Candidate soluble sensitizers to sorafenib effects include cytokines such as interferons or tumor necrosis factor (*e.g.*, produced by immune cells recruited into tumors by JX-594). Apoptosis inhibitors that could be reduced by intratumoral JX-594 effects may include growth factors for cancer cells (*e.g.*, epidermal growth factor) and/or tumor-associated endothelial cells (*e.g.*, VEGF). Of note, we have also demonstrated that targeted oncolytic vaccinia viruses can selectively infect and replicate within tumor-associated endothelial cells but not in normal vasculature.[4] Other investigators have subsequently reported the ability of other viruses to also selectively infect activated tumor-associated endothelial cells.[23] Finally, it is possible that neovasculature forms following JX-594-mediated tumor necrosis and vascular disruption, and that these newly formed vessels are hypersensitive to sorafenib effects.[24] Other vascular disrupting agents are associated with post-treatment increases in angiogenesis. If VEGF signaling is necessary for this phenomenon, other anti-VEGF pathway inhibitors may also be used in combination with JX-594. A pure VEGF pathway inhibitor that does not also inhibit the EGFR/ras/raf pathway would not have the problem of JX-594 replication inhibition that is associated with sorafenib.

Potential safety concerns with this sequential combination therapy should be considered. First, anti-VEGF/VEGFR therapies can cause bleeding from gastrointestinal or pulmonary sites. The JX-594-mediated lysis of tumors that have invaded vital structures might theoretically lead to bleeding, and anti-VEGF therapy might exacerbate this risk. Bleeding complications have not been reported to date with JX-594, but more clinical experience is needed. More patients must be treated in order to adequately assess potential safety risks.

Vaccinia has previously been shown to be inhibited by tyrosine kinase inhibitors such as imatinib (Gleevec, Basel, Switzerland).[25] In particular, vaccinia and other poxviruses are known to exploit activation of the EGFR pathway for their replication and spread from infected cells.[5] Therefore, it is not surprising that inhibitors of this pathway are able to inhibit vaccinia replication.[6] Raf kinase is downstream of ras and the EGF receptor, and its inhibition blocks this signal transduction pathway. Sorafenib was initially discovered because of its raf kinase inhibitory properties.[26] We demonstrate here that sorafenib has antivaccinia properties (>90% inhibition of replication or cytotoxicity *in vitro*) that may make it a useful inhibitor in the case of poxvirus-mediated toxicity. Potential applications include use as an anti-smallpox agent (in the event or reintroduction of the agent into the population), as has been proposed with imatinib, or in the case of live vaccinia virus vaccine complications. In addition, if future replication-mediated toxicities occur with JX-594, sorafenib might be considered in addition to standard antivaccinia agents such as vaccinia immune globulin and cidofovir.

In summary, targeted, oncolytic poxviruses (*e.g.*, JX-594) are novel class of anticancer agents that can be combined with other agents due to their distinct mechanisms-of-action and nonoverlapping toxicity profiles. In particular, therapeutic potential of small-molecule VEGFR inhibitors or other antiangiogenic agents may be enhanced when combined with JX-594 therapy.

MATERIALS AND METHODS

Cell culture and in vitro evaluations. Human tumor cell lines HepG2 (HCC), PLC/PRF/5 (HCC), and A2780 (ovarian) were obtained from American Type Culture Collection (ATCC, Manassas, VA). Additional HCC lines SNU423, SNU475 and SNU449 were obtained from Korea Cell Bank. For evaluation in matched parental and sorafenib-resistant HCC cells, a sorafenib-resistant subclone of PLC/PRF/5 was derived by serial culturing in the presence of increasing concentrations of sorafenib. Sorafenib (Bayer) was dissolved in dimethyl sulfoxide to a concentration of 100 mg/ml and further diluted to appropriate final concentration in Dulbecco's modified Eagle's medium with 10% fetal bovine serum. Dimethyl sulfoxide in the final solution did not exceed 0.1% (v/v). Cells were cultured *in vitro* for a total of 3 months (starting at a sorafenib concentration of 1 μmol/l and increasing up to 6 μmol/l). For plaque formation assays, A2780 or HepG2 cells were seeded into six-well plates at 4×10^5 cells/well and left overnight. Cells were infected with JX-594 for 2 hours, then the media was removed and 3% Carboxymethylcellulose Dulbecco's modified Eagle's medium overlay containing sorafenib at final concentrations of 0–4 μmol/l was added. Three days later, plates were stained with crystal violet and plaques were counted. In parallel, to assess JX-594 replication by Burst Assay (viral one-step growth curve assay), six-well plates were prepared as above. Forty eight hours after viral inoculation, cells were lysed by three rounds of freezing and thawing followed by sonication to release virus; serial dilutions of the crude viral lysate were subsequently

added to A2780 cells to titer the resulting virus by plaque assay. To assess the direct effects of sorafenib on cell viability, cells were plated in 96 well plates and incubated with sorafenib only. Cell viability was determined by means of colorimetric assay based on live-cell mediated reduction of tetrazolium salt to formazan chromogen (Cell Counting Kit-8; Donjindo Laboratories, Kumamoto, Japan).

Murine tumor models. Mice were housed, cared for and used in experiments as approved by the Animal Care and Veterinary Service at the University of Ottawa or by the Ethical Committee for Animal Study at Pusan National University Hospital. The metastatic B16 melanoma murine tumor model was established in C57BL/6 mice by intravenous tail vein infusion of 3×10^5 B16-F10-LacZ cells. Twenty four hours later animals were treated with sorafenib alone (50 µg/kg per oral dosing daily for 2 weeks), JX-594 alone (10^7 pfu intravenously three times per week for 1 week) or in combination ($n = 5$ per group). Three weeks after treatment initiation, mice were killed and lungs were fixed and stained to detect and quantify surface B16 tumor nodules. For the HepG2 xenograft model, female SCID mice were injected subcutaneously with 4×10^5 HepG2 human HCC cells. Once tumors reached a size of ~12–14 mm maximal diameter (within 30 days) mice were randomized into one of six treatment groups ($n = 8$ per group): (i) PBS alone (daily), (ii) sorafenib alone (400 µg intraperitoneally, daily, days 1–31), (iii) intravenous JX-594 alone (10^7 pfu intravenously, weekly, days 1, 8, 15, 22, 29), (iv) simultaneous treatment with JX-594 and sorafenib (daily sorafenib and weekly JX-594, as above), (v) sorafenib (daily, days 1–14) followed by JX-594 (days 15, 22, 29) and (vi) JX-594 (days 1, 8) followed by sorafenib (daily, days 15–31). Tumor measurements were performed every other day until mice were euthanized. Tumor volumes were calculated with the following formula: SD × SD × LD/2. (SD, short diameter; LD, long diameter). Concentrations of sorafenib in the plasma were determined as described previously.[27–29]

Clinical study approvals, consents, and registration. In order to assess effects of addition of sorafenib, three HCC patients who failed to achieve a durable objective tumor response with JX-594 alone were selected for sorafenib therapy after completion of JX-594 treatment. Patients 1702, 1705, and 1712 were treated under a protocol registered at www.clinicaltrials.gov (NCT00554372). Study protocol and informed consent forms were approved by the United States Food and Drug Administration, Korean Food and Drug Administration, and Institutional Review and Infection Control Committees at Pusan National University Hospital, Busan, South Korea. Patient 301 with RCC was treated under a protocol registered at www.clinicaltrials.gov (NCT00629759). Study protocol and informed consent forms were approved by the Korean Food and Drug Administration and Institutional Review and Infection Control Committees at Dong-A University Hospital, Busan, South Korea. Patients signed informed consent according to Good Clinical Practice (GCP) guidelines.

JX-594 treatment procedures and subsequent sorafenib treatment. HCC patients 1702, 1705, and 1712 (NCT00554372) were enrolled and randomized to receive one of two dose levels (10^8 or 10^9 pfu) (**Table 2**). JX-594 was administered *via* imaging-guided intratumoral injection using a multi-pronged Quadrafuse injection needle (RexMedical, Radnor, PA) in roughly spherical tumors, and by a 21-gauge percutaneous ethanol injection (multi-port; HAKKO Medicals, Tokyo, Japan) needle in irregularly shaped tumors and tumors which could not be safely accessed for injection using the Quadrafuse system. Tumors ($n = 1–5$) were injected every 2 weeks for three cycles. The same tumors injected on cycle 1 were injected thereafter on each cycle. After the planned week 8 radiographic analysis, patients 1702, 1705, and 1712 subsequently initiated standard sorafenib dosing (400 mg per oral twice daily) within 2 weeks. All three patients subsequently underwent dose reductions due to grade 1 hand-foot skin reactions (reduced to 400 mg once daily after 52–148 days) (**Table 1**). Sorafenib was eventually discontinued after an additional 1–5 months.

RCC patient 301 treated under protocol NCT00629759 received four doses (1×10^9 pfu per dose) of JX-594 *via* imaging-guided intratumoral injection using a 21-gauge percutaneous ethanol injection, (multi-port; HAKKO Medicals) needle into three intrahepatic target tumors. Patient 301 subsequently received sunitinib at a dose of 50 mg per oral dosing daily. Subsequent dose reductions were carried out after 4 months (decrease to 37.5 mg per day) and 7 months (decrease to 25 mg per day); the rationale for dose reduction was primarily poor wound healing (**Table 1**).

Tumor response and vascularity assessment. Tumor response was assessed prior to sorafenib initiation (at week 8 after JX-594 initiation), and serially over time after sorafenib initiation. Multiphase dynamic contrast-enhanced MRI was performed on either a 1.5T or 3.0T MR system (Siemens, Erlangen, Germany) and using extracellular gadolinium chelate (OptiMARK; Tyco Healthcare, Princeton, NJ). Patient 301 (NCT00629759) was imaged using multiphase dynamic contrast-enhanced computed tomography scanning on a 16-slice multidetector computed tomography scanner (Somatom Plus; Siemens Medical) using nonionic contrast media (Ultravist; Schering, Ansung, Korea). Changes in tumor contrast enhancement, manifested either by signal intensity at MRI or Hounsfield unit density on computed tomography, (and positron emission tomography signal intensity, where applicable) on serial scans were evaluated by a blinded independent radiologist with expertise in liver cancer assessment. Given the mechanism of tumor destruction previously described for JX-594,[9] we elected to apply modified Choi tumor response criteria to assess changes in tumor density and perfusion. Modified Choi responses were defined as a decrease in tumor density of ≥15% and/or a decrease in maximum diameter of ≥10%.[15]

3D segmentation analysis methods. The software used to create the 3D models was developed by M2S (Lebanon, NH). The input data comprised the arterial phase of dynamic contrast-enhanced MRI scan performed with a 3D spoiled gradient echo pulse sequence. Three tumors were selected for 3D segmentation analysis using software which allows for variable threshholding based on signal intensity. A radiologist with expertise in evaluating HCC on MRI then evaluated the liver lesions for necrosis versus viable tissue, and instructed an imaging specialist to set the thresh holds for each of these two compartments. A 3D model of the whole liver based using the edge-detection capabilities of the software was subsequently generated.

Manufacturing and preparation of JX-594. JX-594 is a Wyeth strain vaccinia modified by insertion of the human *GM-CSF* and *Lac-Z* genes into the vaccinia *TK* gene region under control of the synthetic early late promoter and p7·5 promoter, respectively. Clinical trial material was generated according to Good Manufacturing Practice guidelines in Vero cells and purified through sucrose gradient centrifugation. The genome-to-pfu ratio was ~70:1. JX-594 was formulated in phosphate-buffered saline with 10% glycerol, 138 mmol/l sodium chloride at pH 7.4. Final product quality control release tests included assays for sterility, endotoxin, and potency. Clinical trial material was also tested for GM-CSF protein concentration and was negative (lower limit of detection <14,000 pg/ml). JX-594 was diluted in 0·9% buffered normal saline in a volume equivalent to 25% (NCT00629759) or 50% (NCT00554372) of the estimated total volume of target tumor(s) for intratumoral injection.

Statistical analysis. The difference in tumor volume in mice over time was compared using the paired Student's *t*-test. The statistical analysis for the time-to-tumor progression was performed using Kaplan–Meier estimates and the log-rank test. Differences in the number of lung metastases were assessed using the unpaired *t*-test using GraphPad Prism 5 software (GraphPad, La Jolla, CA).

REFERENCES

1. Kim, JH, Oh, JY, Park, BH, Lee, DE, Kim, JS, Park, HE *et al.* (2006). Systemic armed oncolytic and immunologic therapy for cancer with JX-594, a targeted poxvirus expressing GM-CSF. *Mol Ther* **14**: 361–370.
2. Caux, C, Dezutter-Dambuyant, C, Schmitt, D and Banchereau, J (1992). GM-CSF and TNF-alpha cooperate in the generation of dendritic Langerhans cells. *Nature* **360**: 258–261.
3. Breitbach, CJ, Paterson, JM, Lemay, CG, Falls, TJ, McGuire, A, Parato, KA *et al.* (2007). Targeted inflammation during oncolytic virus therapy severely compromises tumor blood flow. *Mol Ther* **15**: 1686–1693.
4. Kirn, DH, Wang, Y, Le Boeuf, F, Bell, J and Thorne, SH (2007). Targeting of interferon-beta to produce a specific, multi-mechanistic oncolytic vaccinia virus. *PLoS Med* **4**: e353.
5. Katsafanas, GC and Moss, B (2004). Vaccinia virus intermediate stage transcription is complemented by Ras-GTPase-activating protein SH3 domain-binding protein (G3BP) and cytoplasmic activation/proliferation-associated protein (p137) individually or as a heterodimer. *J Biol Chem* **279**: 52210–52217.
6. Yang, H, Kim, SK, Kim, M, Reche, PA, Morehead, TJ, Damon, IK *et al.* (2005). Antiviral chemotherapy facilitates control of poxvirus infections through inhibition of cellular signal transduction. *J Clin Invest* **115**: 379–387.
7. Stojdl, DF, Lichty, B, Knowles, S, Marius, R, Atkins, H, Sonenberg, N *et al.* (2000). Exploiting tumor-specific defects in the interferon pathway with a previously unknown oncolytic virus. *Nat Med* **6**: 821–825.
8. Hengstschläger, M, Pfeilstöcker, M and Wawra, E (1998). Thymidine kinase expression. A marker for malignant cells. *Adv Exp Med Biol* **431**: 455–460.
9. Park, BH, Hwang, T, Liu, TC, Sze, DY, Kim, JS, Kwon, HC *et al.* (2008). Use of a targeted oncolytic poxvirus, JX-594, in patients with refractory primary or metastatic liver cancer: a phase I trial. *Lancet Oncol* **9**: 533–542.
10. Liu, TC, Hwang, T, Park, BH, Bell, J and Kirn, DH (2008). The targeted oncolytic poxvirus JX-594 demonstrates antitumoral, antivascular, and anti-HBV activities in patients with hepatocellular carcinoma. *Mol Ther* **16**: 1637–1642.
11. Wilhelm, SM, Carter, C, Tang, L, Wilkie, D, McNabola, A, Rong, H *et al.* (2004). BAY 43-9006 exhibits broad spectrum oral antitumor activity and targets the RAF/MEK/ERK pathway and receptor tyrosine kinases involved in tumor progression and angiogenesis. *Cancer Res* **64**: 7099–7109.
12. Llovet, JM, Ricci, S, Mazzaferro, V, Hilgard, P, Gane, E, Blanc, JF *et al.*; SHARP Investigators Study Group. (2008). Sorafenib in advanced hepatocellular carcinoma. *N Engl J Med* **359**: 378–390.
13. Cheng, AL, Kang, YK, Chen, Z, Tsao, CJ, Qin, S, Kim, JS *et al.* (2009). Efficacy and safety of sorafenib in patients in the Asia-Pacific region with advanced hepatocellular carcinoma: a phase III randomised, double-blind, placebo-controlled trial. *Lancet Oncol* **10**: 25–34.
14. Lencioni, R and Llovet, JM (2010). Modified RECIST (mRECIST) assessment for hepatocellular carcinoma. *Semin Liver Dis* **30**: 52–60.
15. Choi, H, Charnsangavej, C, Faria, SC, Macapinlac, HA, Burgess, MA, Patel, SR *et al.* (2007). Correlation of computed tomography and positron emission tomography in patients with metastatic gastrointestinal stromal tumor treated at a single institution with imatinib mesylate: proposal of new computed tomography response criteria. *J Clin Oncol* **25**: 1753–1759.
16. Abou-Alfa, GK, Schwartz, L, Ricci, S, Amadori, D, Santoro, A, Figer, A *et al.* (2006). Phase II study of sorafenib in patients with advanced hepatocellular carcinoma. *J Clin Oncol* **24**: 4293–4300.
17. Therasse, P, Arbuck, SG, Eisenhauer, EA, Wanders, J, Kaplan, RS, Rubinstein, L *et al.* (2000). New guidelines to evaluate the response to treatment in solid tumors. European Organization for Research and Treatment of Cancer, National Cancer Institute of the United States, National Cancer Institute of Canada. *J Natl Cancer Inst* **92**: 205–216.
18. Patil, S, Figlin, RA, Hutson, TE, Michaelson, MD, Négrier, S, Kim, ST *et al.* (2010). Prognostic factors for progression-free and overall survival with sunitinib targeted therapy and with cytokine as first-line therapy in patients with metastatic renal cell carcinoma. *Ann Oncol* **22**:295–300.
19. Breitbach, CJH, Cho, M, Jun, W, Woo, W, Yon, K, Hwang, T-H *et al* (2010). Evaluating safety and antitumoral activity of JX-594, a targeted multi-mechanistic oncolytic poxvirus, followed by sorafenib therapy in patients with advanced hepatocellular carcinomaL pilot study for Phase 3. In *International Liver Cancer Association Fourth Annual Conference*, Montreal, Canada.
20. Kim, J, Kim, JY, Song, KS, Lee, YH, Seo, JS, Jelinek, J *et al.* (2007). Epigenetic changes in estrogen receptor beta gene in atherosclerotic cardiovascular tissues and in-vitro vascular senescence. *Biochim Biophys Acta* **1772**: 72–80.
21. El-Osta, A, Brasacchio, D, Yao, D, Pocai, A, Jones, PL, Roeder, RG *et al.* (2008). Transient high glucose causes persistent epigenetic changes and altered gene expression during subsequent normoglycemia. *J Exp Med* **205**: 2409–2417.
22. Kim, JY, Hwang, JH, Zhou, W, Shin, J, Noh, SM, Song, IS *et al.* (2009). The expression of VEGF receptor genes is concurrently influenced by epigenetic gene silencing of the genes and VEGF activation. *Epigenetics* **4**: 313–321.
23. Kottke, T, Hall, G, Pulido, J, Diaz, RM, Thompson, J, Chong, H *et al.* (2010). Antiangiogenic cancer therapy combined with oncolytic virotherapy leads to regression of established tumors in mice. *J Clin Invest* **120**: 1551–1560.
24. Plastaras, JP, Kim, SH, Liu, YY, Dicker, DT, Dorsey, JF, McDonough, J *et al.* (2007). Cell cycle dependent and schedule-dependent antitumor effects of sorafenib combined with radiation. *Cancer Res* **67**: 9443–9454.
25. Reeves, PM, Bommarius, B, Lebeis, S, McNulty, S, Christensen, J, Swimm, A *et al.* (2005). Disabling poxvirus pathogenesis by inhibition of Abl-family tyrosine kinases. *Nat Med* **11**: 731–739.
26. Lyons, JF, Wilhelm, S, Hibner, B and Bollag, G (2001). Discovery of a novel Raf kinase inhibitor. *Endocr Relat Cancer* **8**: 219–225.
27. Jain, L, Gardner, ER, Venitz, J, Dahut, W and Figg, WD (2008). Development of a rapid and sensitive LC-MS/MS assay for the determination of sorafenib in human plasma. *J Pharm Biomed Anal* **46**: 362–367.
28. Zhao, M, Rudek, MA, He, P, Hafner, FT, Radtke, M, Wright, JJ *et al.* (2007). A rapid and sensitive method for determination of sorafenib in human plasma using a liquid chromatography/tandem mass spectrometry assay. *J Chromatogr B Analyt Technol Biomed Life Sci* **846**: 1–7.
29. Afify, S, Rapp, UR and Högger, P (2004). Validation of a liquid chromatography assay for the quantification of the Raf kinase inhibitor BAY 43-9006 in small volumes of mouse serum. *J Chromatogr B Analyt Technol Biomed Life Sci* **809**: 99–103.